


Sensitivity to supernovae average ν_x temperature with neutral current interactions in DUNE

Darcy A. Newmark¹ and Austin Schneider^{2,1}

¹*Department of Physics, Massachusetts Institute of Technology, Cambridge, Massachusetts 02139, USA*

²*Los Alamos Laboratory, Los Alamos, New Mexico 87545, USA*

 (Received 12 April 2023; accepted 14 July 2023; published 7 August 2023)

We explore a novel method for measuring the time averaged temperature of the ν_x component in type-II core-collapse supernovae. By measuring neutral current incoherent neutrino-argon interactions in DUNE we can obtain spectral information for the combination of all active neutrino species. Combining this all-neutrino spectral information with detailed charged current measurements of the electron neutrino and electron antineutrino fluxes from DUNE and Hyper-Kamiokande, we can infer the time averaged temperature for the remaining neutrino species in the ν_x component to within a factor 2 for most cases and to 30% for a small range of time averaged ν_x temperatures. Because of the limited energy range of the emitted photons from incoherent neutral current interactions on argon, the ν_x temperature reconstruction demonstrates a degeneracy in the one and two sigma credible regions. Furthermore, while large uncertainties on the neutral current (NC) cross section penalize this measurement, we examined the efficacy of constraining NC cross section uncertainties on improving ν_x measurements. We found that if additional measurements of $B(M1 \uparrow) 1^+$ excited state transitions in argon are able to reduce correlated cross section uncertainties from 15% to 7%, the size of the 1σ allowed regions for T_{ν_x} becomes sample size limited, and approaches the case where there are no uncertainties on the cross section.

DOI: [10.1103/PhysRevD.108.043005](https://doi.org/10.1103/PhysRevD.108.043005)

I. INTRODUCTION

Type-II core-collapse supernova events release approximately 10^{53} ergs of energy, carried away almost exclusively by neutrinos and antineutrinos of all flavors [1]. These neutrinos travel nearly unimpeded to Earth, where they can be detected. In 1987, three neutrino detectors on Earth measured 20 events within 13 seconds, which coincided with the release of energy from the collapse of SN1987A [2–4]. If a core-collapse supernova event were to occur within our Galaxy today, the many operating neutrino detectors would provide precise measurements of neutrino and antineutrino energy spectra. Such measurements are crucial for reconstructing the initial conditions of supernovae just before collapse, understanding their evolution, and modeling their collapse.

Large detectors such as the Deep Underground Neutrino Experiment (DUNE) and Hyper-Kamiokande (Hyper-K) will provide large sample measurements of ν_e and $\bar{\nu}_e$ charged current (CC) interactions, respectively, with

excellent energy resolution [5,6]. However, the remaining neutrino species, summarized as ν_x , are below threshold for CC interactions and can only be measured through neutral current (NC) interactions. While there are many theoretical models of supernova collapse, they vary greatly in the prediction and treatment of ν_x [7–9]. With little existing experimental information and large uncertainties in the model space, measurements of NC neutrino interactions will be crucial for understanding the ν_x component of core-collapse supernovae.

In this paper, we explore how DUNE’s observation of gamma rays generated by NC interactions of supernova neutrinos can be used in conjunction with CC observations to infer the time averaged temperature of the supernova ν_x component. NC interactions of all supernova neutrino species in DUNE will excite argon nuclei, which subsequently emit a gamma ray at one of several known energies, providing a weak correlation between incident neutrino energy and the emitted gamma-ray energies. We then combine the flavor-agnostic measurement of this NC gamma-ray spectrum with CC spectral measurements of the ν_e and $\bar{\nu}_e$ components to infer the temperature of the ν_x component. We also explore how uncertainties in the NC cross section impact sensitivity to the ν_x temperature, using recently updated calculations of the NC neutrino-nucleus cross section and its associated uncertainties [10].

Published by the American Physical Society under the terms of the Creative Commons Attribution 4.0 International license. Further distribution of this work must maintain attribution to the author(s) and the published article’s title, journal citation, and DOI. Funded by SCOAP³.

II. NEUTRAL CURRENT MEASUREMENTS

In order to examine DUNE's sensitivity to supernova ν_x temperature reconstruction, we must first consider the signatures of the NC interaction channel.

In the incoherent NC interaction, argon nuclei are excited via interaction with a neutrino. As the nucleus deexcites, γ rays are emitted at specific energy levels. The magnetic dipole strengths of these 1^+ excited state transitions are displayed in Fig. 1. These measurements, combined with shell model calculations, guide neutral current cross section predictions and dictate experimental reconstruction of incident neutrino spectra.

NC neutrino-argon interactions are difficult to measure due to the small cross section of this channel and low energy at which the interactions occur [10]. For supernova neutrino energies, the NC interaction cross section is at least 2 orders of magnitude smaller than the corresponding CC cross section, given by [11]. For this reason, projected measurements of supernova neutrinos tend to focus on CC channels.

While NC measurements are difficult to make compared to the CC channel, they provide the only source of information about the neutrino species of ν_x . Flavor nonspecific information from supernova neutrinos is crucial to understanding the neutrino flux emitted without uncertainties related to neutrino oscillations, matter effects, or neutrino self-interactions that occur within the supernovae. Combining flavor nonspecific NC measurements with ν_e and $\bar{\nu}_e$ CC measurements, we can indirectly probe the properties of the supernova ν_x flux.

Recent developments in detector technology will allow us to overcome this challenge with ultralarge detectors that are sensitive to these low energy NC interactions. With 40 kt of combined fiducial mass and energy resolution down to the MeV scale, the DUNE far detector (FD) modules will be an ideal candidate to study the ν_x component, providing the

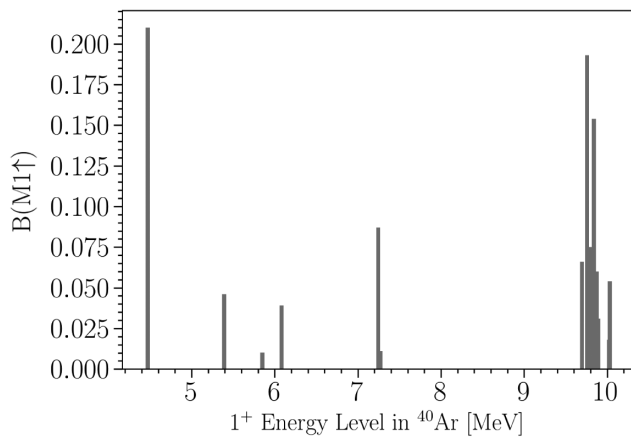


FIG. 1. $B(M1\uparrow)$ neutral current 1^+ transition strengths for ^{40}Ar . The $B(M1\uparrow)$ value for each 1^+ is shown as a function of the transition energy. Fourteen of these 1^+ transitions exist in total.

largest sample of NC neutrino-argon interactions [12]. DUNE will be able to separate CC from NC interactions using the distribution of deposited energy as a function of interaction length within the detector. The DUNE FD modules are planned to have a high efficiency trigger system down to the few MeV threshold, with good energy resolution, and moderate spatial resolution [12,13]. With these anticipated capabilities, DUNE will be able to resolve photon emissions from NC interactions in the energy range of interest for this analysis.

While this work is directly relevant to DUNE, SBND, ICARUS and other liquid argon (LAr) detectors, supernova neutrino interaction measurements on other nuclei will provide further insights into the ν_x spectrum. The Jiangmen Underground Neutrino Observatory (JUNO) experiment will be able to observe incoherent neutral current neutrino interactions on carbon nuclei, with a predominant excitation state of 15.1 MeV [14]. With a 20 kt fiducial mass of liquid scintillator and excellent energy resolution of $3\%/\sqrt{E(\text{MeV})}$, JUNO is another large neutrino detector that will be sensitive to the NC channel from supernova neutrinos [14]. Given the different photon excitation energies of NC neutrino-nucleus interactions on argon and carbon, a combined analysis of NC neutrino interactions on ^{40}Ar and ^{12}C would be sensitive to greater parameter space than either individual analyses. This combined analysis of data from DUNE and JUNO could provide a more robust and more sensitive measurement of ν_x supernova neutrinos than either individual analysis.

In addition to NC measurements, DUNE and Hyper-K will provide leading constraints on the ν_e and $\bar{\nu}_e$ spectrum through CC measurements on liquid argon and water, respectively. By incorporating DUNE CC, DUNE NC, and Hyper-K CC measurements in a combined analysis, we can make definitive statements about the ν_x component of the neutrino flux. Although sample sizes for NC events are much smaller, and energy resolution is poorer, the information we obtain from NC interaction on argon nuclei in DUNE provides enough discriminating power to reconstruct the time averaged ν_x temperature.

III. METHODOLOGY

Modeling the expected neutral current event rate requires (1) the supernova neutrino spectrum, (2) the neutrino-nucleon NC interaction cross section, (3) the detector response of DUNE's far detector modules, and (4) an event selection.

For the supernova neutrino spectrum, we assume a representative supernova neutrino flux with a progenitor mass of ten solar masses, a distance of 10 kpc, and a Fermi-Dirac energy spectrum [15] given by

$$\frac{dF_\nu}{d\varepsilon_\nu} = \frac{L_\nu}{4\pi D^2 T_\nu^4 F_3(\eta)} \frac{\varepsilon_\nu^2}{e^{\beta(\varepsilon_\nu - \mu)} + 1}, \quad (1)$$

where ε_ν is incident neutrino energy, L_ν is the luminosity for each neutrino species of SN1987A integrated over total time of collapse for a total energy of approximately 3×10^{53} ergs, D is the distance from Earth to the supernova, T_ν is the time averaged temperature of the neutrino species, μ is the chemical potential, $\beta = 1/T_\nu$, and $\eta = \mu/T_\nu$ (the Boltzmann constant is set to unity). $F_3(\eta)$ is defined by

$$F_3(\eta) \equiv \int_0^\infty \frac{x^3}{e^{x-\eta} + 1} dx, \quad (2)$$

and in this work η is set to 0. Figure 2 provides an example of this calculation, setting $T_{\nu_e} = 3.3$ MeV, $T_{\bar{\nu}_e} = 4.6$ MeV, and $T_{\nu_x} = 6.4$ MeV. Because the NC interaction is flavor independent, we compute the fluence assuming a no neutrino oscillation scenario. In this work we neglect further modification of the spectrum from a pinching parameter [1,7–9,16] because such features in the energy spectrum will not be resolvable in the ν_x component through NC measurements.

For the neutrino-nucleon NC interaction cross section, we use the most recently published NC cross sections from W. Tornow *et al.* [10]. Figure 3 shows this cross section for neutrinos and antineutrinos with 43% theoretical uncertainty. We model the NC cross section uncertainties as a 15% correlated uncertainty within each excitation mode, corresponding to the uncertainty on $B(M1\uparrow)$ measurements, and an additional 40% uncorrelated uncertainty across the entire energy spectrum to account for the theoretical uncertainties between different choices of shell-model calculations. Figure 4 shows an example fractional covariance matrix used in this calculation.

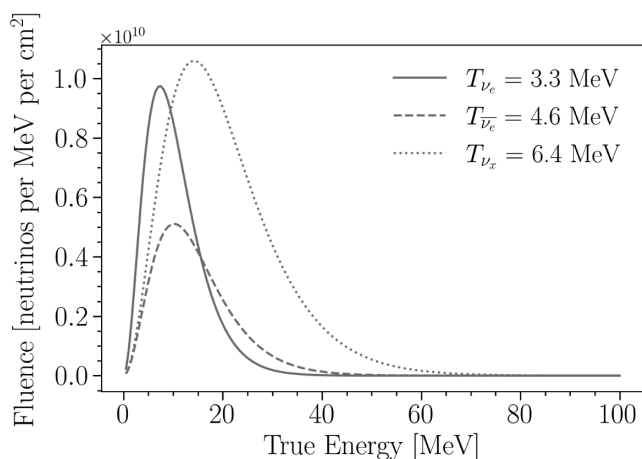


FIG. 2. Supernova neutrino differential fluence for a Fermi-Dirac spectrum. The differential fluence is shown as a function of neutrino energy for each of the three neutrino flux components, assuming a Fermi-Dirac energy distribution, and the baseline supernova scenario described in Sec. III.

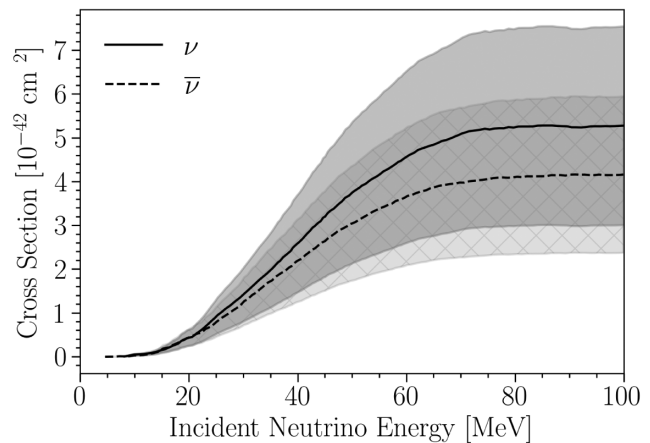


FIG. 3. Incoherent NC neutrino-argon cross sections and uncertainties. The NC neutrino-argon cross sections derived in [10] are shown for ν and $\bar{\nu}$ as a function of incident neutrino energy with bands showing their associated 43% theoretical uncertainties. The solid shading shows ν cross section uncertainties, and hatched shading shows the same for $\bar{\nu}$.

For the detector response of DUNE’s far detector modules, we assume the 15% photon energy resolution expected in DUNE’s Time Projection Chambers (TPCs) at the energies of relevance for supernova neutrino measurements [12]. We also note that variation in the detectors response to NC neutrino interactions of different incident neutrino energies predominantly arises from the threshold of different nuclear excitations and changes in the branching ratio of these same excitations. Using this predicted energy resolution and weighting it by the cross sections of the individual photon excitation modes, Fig. 5 shows the response matrix for the ν component of the NC cross section.

Finally, for the event selection, we consider the relevant background processes for NC events and choose

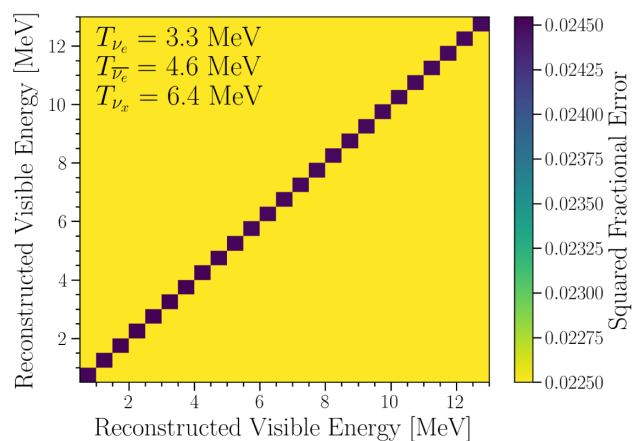


FIG. 4. DUNE FD NC fractional covariance matrix. The uncertainties on the cross section are composed of 15% correlated uncertainties and 40% uncorrelated uncertainties, as described in [10].

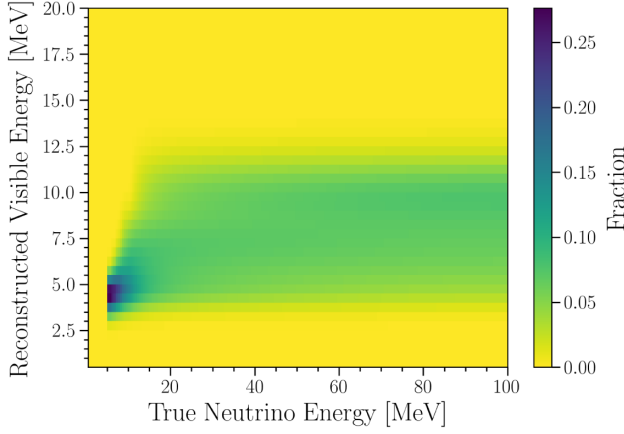


FIG. 5. DUNE FD NC response matrix. Response matrix for the ν component of the incoherent NC neutrino interaction in LAR assuming 15% energy resolution for the DUNE FD TPC as described in [12].

appropriate cuts to model the signal and background efficiencies. In the DUNE far detector modules, the primary background for NC interactions from supernova neutrinos is CC interactions from the ν_e neutrino flux. These CC interactions mostly occur at energies above the energy of the photons from NC interactions, and so we restrict our discussion of the CC background to reconstructed visible energies between 0.5 and 13 MeV. The electrons produced in CC interactions can be further differentiated from the photons produced in NC interactions using the fine grained information available from the LAR TPC. For simplicity we assume that most of this selection power is captured in the dE/dx distribution. Figure 6 shows the simulated dE/dx distributions, described in [12], scaled to the expected event rates of the NC and CC channels within the reconstructed energy region of interest between 0.5 and 13 MeV for $T_{\nu_e} = 3.3$ MeV, $T_{\bar{\nu}_e} = 4.6$ MeV, and $T_{\nu_x} = 6.4$ MeV. We

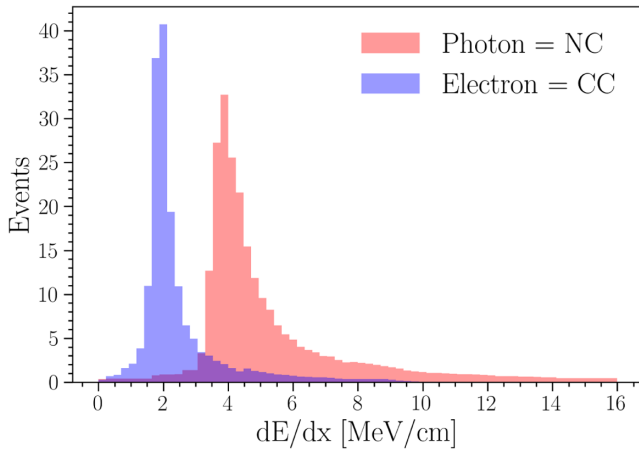


FIG. 6. DUNE dE/dx distribution for electron and photonlike final states. Distribution is normalized to the expected NC and CC event rates for a representative sample where $T_{\nu_x} = 3.3$ MeV, $T_{\bar{\nu}_e} = 4.6$ MeV, and $T_{\nu_x} = 6.4$ MeV.

found that a single cut at $dE/dx = 3.1$ MeV/cm includes 95.26% of NC signal events, while rejecting all but 15.83% of background CC interactions from the ν_e supernova neutrino flux.

Figure 7 shows an example of the expected reconstructed event rate in DUNE FD, after combining the fluence for the specified neutrino temperatures, NC cross section, response matrix, and efficiency cut. This plots shows the expected events for $T_{\nu_e} = 3.3$ MeV and $T_{\bar{\nu}_e} = 4.6$ MeV while T_{ν_x} varies between 1 and 30 MeV. The dashed black line represents the CC events due to the ν_e component of the supernova neutrino flux in DUNE. Although the NC channel is suppressed compared to the CC channel, DUNE's large detector size combined with the high fluence of expected neutrinos for a supernova collapse provides us with a large enough sample to perform spectral analysis.

With the modeling of DUNE's NC measurements complete, we must now combine this flavor-agnostic information with the CC measurements of the ν_e and $\bar{\nu}_e$ temperatures from DUNE and Hyper-K, respectively. This combination of three measurements will allow us to infer the temperature of the ν_x component. DUNE TPCs are predicted to resolve energies in the ν_e CC region of interest to around 15% [12]. Using this energy resolution to calculate the CC response matrix, ν_e fluence described in Eq. (1), and CC cross section [11], we calculate the predicted CC event rate as a function of ν_e temperature in DUNE and are able to reconstruct injected temperatures to 1σ credible region with 0.5% fractional error. We expect that Hyper-K will be able to reconstruct the $\bar{\nu}_e$ temperature to similar precision, if not better, given their similar energy resolution [17] as the DUNE TPC, greater fiducial mass [18] than the DUNE FD modules, and greater cross section for inverse beta decay events below ~ 15 MeV than ν_e CC events on argon [19].

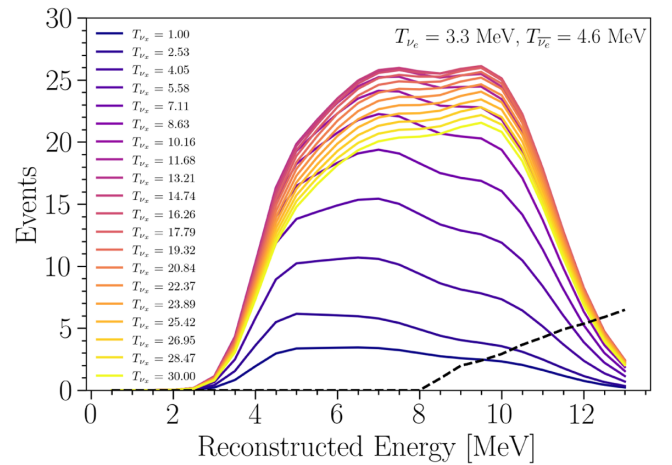


FIG. 7. Expected NC event rate in DUNE FD as a function of ν_x temperature. ν_e and $\bar{\nu}_e$ temperatures are fixed to 3.3 and 4.6 MeV, respectively. The black dashed line represents events due to CC interactions in the DUNE FD from the ν_e component of the fluence.

IV. STATISTICAL METHODS

With the methods described above, we can now predict the NC event rates in DUNE for any combination of temperatures of the three neutrino flux components. The NC data from DUNE provides information about the total neutrino flux, however, to obtain sensitivity to the ν_x temperature we must simultaneously constrain the temperature of the ν_e and $\bar{\nu}_e$ components. We construct the binned-log-likelihood comparing expected NC DUNE data to our predictions, and combine this with external statistical constraints on ν_e and $\bar{\nu}_e$. This combination produces a constrained log likelihood given by

$$\mathcal{L}(\vec{T}) = \left[\prod_i \frac{\lambda_i(\vec{T}, \alpha_i)^{k_i} e^{-\lambda_i(\vec{T}, \alpha_i)}}{k_i!} \right] \mathcal{P}(T_{\nu_e}) \mathcal{P}(T_{\bar{\nu}_e}) \mathcal{P}(\vec{\alpha}), \quad (3)$$

where $\lambda_i(\vec{T}, \alpha_i)$ is the expected number of events in bin i for the combination of temperatures \vec{T} , and k_i is the number of observed data events in bin i . For the two external constraints, $\mathcal{P}(T_{\nu_e})$ and $\mathcal{P}(T_{\bar{\nu}_e})$, we assume normally distributed constraints centered on the true values of the temperatures with widths that correspond to the uncertainties on ν_e and $\bar{\nu}_e$ temperatures that we expect to obtain from the CC measurements of DUNE and Hyper-K, conservatively assumed to be 0.5%. To model the cross section uncertainties, we introduce the parameters $\vec{\alpha}$ which fractionally modify the expected number of events in each bin, such that $\lambda_i(\vec{T}, \alpha_i) = (1 + \alpha_i) \cdot \lambda_i(\vec{T})$. The parameters $\vec{\alpha}$ are constrained by the multivariate normal distribution denoted by $\mathcal{P}(\vec{\alpha})$, which has a fractional covariance matrix derived from the cross section uncertainties.

To explore the sensitivity of this combined analysis to the ν_x timed averaged temperature, we examine a set of representative scenarios where $T_{\nu_e} = 3.3$ MeV, $T_{\bar{\nu}_e} = 4.6$ MeV, and T_{ν_x} has a value between 0.5 and 30 MeV. For each value of T_{ν_x} we perform an Asimov test, where the nominal expected event distribution is injected as data. We use a Markov chain Monte Carlo with adaptive parallel tempering [20,21] to explore the parameter space, and derive Bayesian credible regions (CRs) for T_{ν_x} that are marginalized over T_{ν_e} , $T_{\bar{\nu}_e}$, and the nuisance parameters $\vec{\alpha}$. The two electron flavor temperatures have normal priors modeled after the expected constraints from CC data, and the nuisance parameters $\vec{\alpha}$ have a multivariate-normal prior, as described in Eq. (3). We use a uniform prior for T_{ν_x} across most of the parameter space, but introduce a hyperbolic tangent cutoff at 60 MeV, with a characteristic transition width of 3 MeV. For injected T_{ν_x} less than 10 MeV a degenerate region of the parameter space becomes apparent, which extends to reconstructed temperatures above 100 MeV for the lowest injected temperatures. We focus the results presented here on temperatures below 60 MeV, because such large temperatures are not within the expected range, and will be ruled out by other

observations [22–27]. This is accomplished with the hyperbolic tangent cutoff, the primary effect of which is a reduction in the size of the derived CRs for injected T_{ν_x} less than 5 MeV, because there is no longer appreciable posterior mass above 60 MeV. Additional discussion of this prior, and CRs derived with a uniform T_{ν_x} prior from 0.1 to 300 MeV are given in the Appendix.

V. RESULTS

The time averaged ν_e and $\bar{\nu}_e$ temperatures will be constrained very well by CC measurements from DUNE and Hyper-K. As a result, the sensitivity to T_{ν_x} does not significantly depend on the choice of injected T_{ν_e} and $T_{\bar{\nu}_e}$. We can therefore examine the sensitivity to reconstructed ν_x temperature as a function of true injected ν_x temperature without significant bias from the choice of injected ν_e and $\bar{\nu}_e$ temperatures. We present sensitivities to T_{ν_x} , using $T_{\nu_e} = 3.3$ MeV and $T_{\bar{\nu}_e} = 4.6$ MeV as a representative set of temperatures.

We explore sensitivities for three scenarios with different cross section uncertainties: a case without cross section uncertainties, a case with full cross section uncertainties, and a case with reduced cross section uncertainties. The case with full cross section uncertainties assumes 40% fully uncorrelated uncertainty in the cross section and a 15% correlated uncertainty in the cross section as described in Sec. III. The case with reduced cross section uncertainties retains the 40% fully uncorrelated uncertainty, but reduces the correlated uncertainty to 7% to model the effect of improved B(M1 \uparrow) measurements. Figures 8–10 show the expected sensitivity to T_{ν_x} as Asimov credible regions for

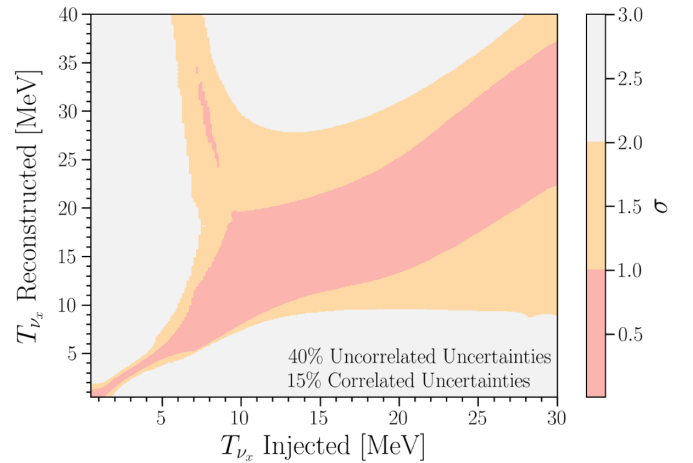


FIG. 8. Expected T_{ν_x} credible regions with full cross section uncertainties. The Asimov credible regions for T_{ν_x} are shown as a function of injected T_{ν_x} by the colored regions. Average neutrino temperatures of $T_{\nu_e} = 3.3$ MeV and $T_{\bar{\nu}_e} = 4.6$ MeV are assumed, along with 40% uncorrelated uncertainties and 15% correlated uncertainties on the NC cross section.

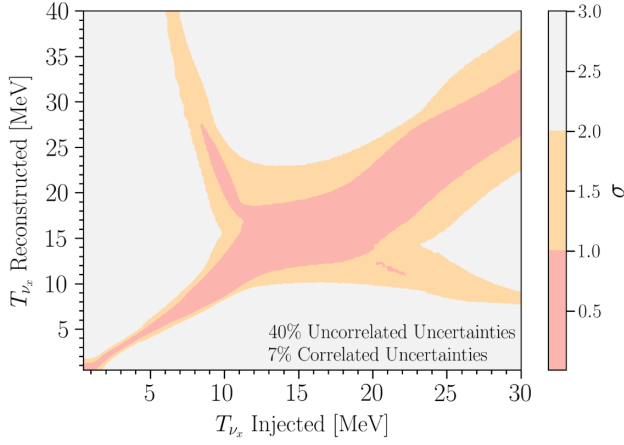


FIG. 9. Expected T_{ν_x} credible regions with reduced cross section uncertainties. The Asimov credible regions for T_{ν_x} are shown as a function of injected T_{ν_x} by the colored regions. Average neutrino temperatures of $T_{\nu_e} = 3.3$ MeV and $T_{\bar{\nu}_e} = 4.6$ MeV are assumed, along with 40% uncorrelated uncertainties and 7% correlated uncertainties on the NC cross section.

the no uncertainty, full uncertainty, and reduced uncertainty cases, respectively.

There are two distinct degenerate regions that arise in the measurement space from multiple factors. The primary cause is the discrete γ -ray energies of the NC cross section that results in a decoupling between neutrino energy and observed energy. In addition to that, for T_{ν_x} above approximately 8 MeV the total fluence becomes much more uniform across the energy range of the NC excitations. These characteristics of the NC cross section combined with the Fermi-Dirac spectrum at higher temperatures leads to a degeneracy in the ν_x temperature measurement.

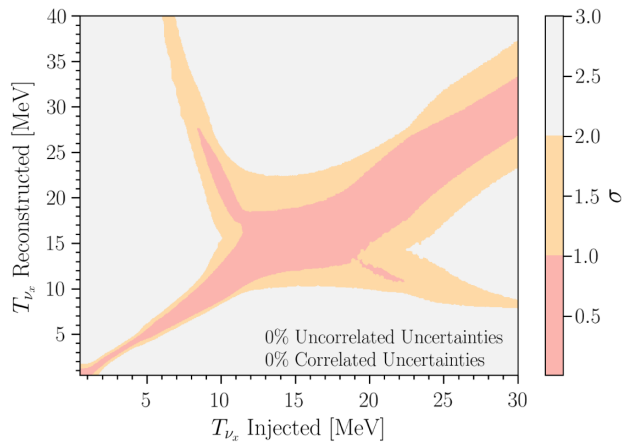


FIG. 10. Expected T_{ν_x} credible regions with no cross section uncertainties. The Asimov credible regions for T_{ν_x} are shown as a function of injected T_{ν_x} by the colored regions. Average neutrino temperatures of $T_{\nu_e} = 3.3$ MeV and $T_{\bar{\nu}_e} = 4.6$ MeV are assumed, along with no uncertainties on the NC cross section.

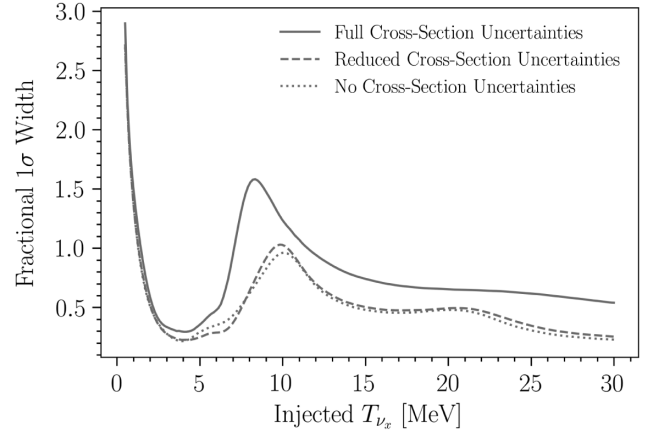


FIG. 11. Fractional width of the 1σ credible region. The solid line represents the scenario with 40% uncorrelated uncertainties and 15% correlated uncertainties on the NC cross section. The dashed line represents the scenario with 40% uncorrelated uncertainties and 7% correlated uncertainties on the NC cross section. The dotted line represents the scenario with no uncertainties on the NC cross section.

Figure 11 shows the fractional width of the 1σ credible region for these measurements. The peak in the fractional width of the 1σ credible region around 10 MeV true ν_x temperature is due to the degeneracy in the measurement. Reducing the correlated uncertainties from 15% to 7%, without changes to the 40% uncorrelated uncertainties, reduces the fractional width of the 1σ credible region almost to that of the measurement without any uncertainties on the cross section. This demonstrates that even modest improvements to the argon B(M1 \uparrow) measurements provide substantial improvements to the T_{ν_x} sensitivity.

VI. CONCLUSIONS

While NC channel measurements of supernova neutrinos are often overlooked due to the technical challenges and small sample sizes, this analysis has shown the power of NC measurements in measuring ν_x spectral information from type-II core-collapse supernova events. Because of the discrete excitation nature of this interaction channel, the energy spectrum from supernova neutrinos cannot be resolved, but general parameters of the fluence can be measured to the 1σ and 2σ level. For this analysis we focused on measuring the time averaged ν_x temperature from the incoherent NC neutrino-argon interaction in the DUNE FD modules. To make this measurement we combined the expected incoherent NC sample from the DUNE FD with expected constraints from the CC channel measurements of the DUNE and Hyper-K experiments on T_{ν_e} and $T_{\bar{\nu}_e}$ of the supernova flux. We find that such a combined analysis can measure the ν_x temperature to within a factor of 2 in most cases, and to within 30% in the best case.

In addition to exploring DUNE's sensitivity to time averaged ν_x temperature using the NC channel, we explore

the effects of reducing the uncertainty in NC cross section predictions. By reducing correlated uncertainties from 15% to 7%, the T_{ν_x} measurement becomes sample size limited, and approaches the case where there are no uncertainties on the cross section. More precise measurements of $B(M1\uparrow)$ transition strengths will provide even greater spectral information for the ν_x component of supernova flux. While this measurement will be limited by the small energy range of argon-nucleus gamma emissions from NC interactions, combining NC measurements of neutrinos on argon with NC measurements of neutrinos on carbon from JUNO could provide stronger constraints on time averaged ν_x temperature.

ACKNOWLEDGMENTS

We want to thank Janet M. Conrad for insights on liquid argon TPCs. We would also like to thank Anna C. Hayes for her dedicated work on modeling neutral current cross sections. D. A. N. is supported by the NSF Graduate Research Fellowship under Grant No. 2141064. A. S. is supported by the U.S. Department of Energy through the Los Alamos National Laboratory. Los Alamos National Laboratory is

operated by Triad National Security, LLC, for the National Nuclear Security Administration of U.S. Department of Energy (Contract No. 89233218CNA000001).

APPENDIX: T_{ν_x} PRIOR

In this work we demonstrate the potential sensitivity of the DUNE FD to the time averaged temperature of the supernova ν_x component with credible regions derived from the highest posterior density regions (HPDs). A side effect of this methodology is a dependence of the local HPD width on the global distribution of posterior mass. For these NC derived constraints on T_{ν_x} , a degenerate region of allowed ν_x temperatures is present for the entire energy range. Below ~ 10 MeV and above ~ 20 MeV, this degeneracy manifests as two distinct allowed regions at both the 1σ and 2σ level. For some values of injected T_{ν_x} the allowed region not centered on the injected temperature, referred to as the degenerate region, lies within the range of expected supernova neutrino temperatures. However, for injected T_{ν_x} less than ~ 5 MeV this degenerate region exists at temperatures far above the expected range of supernova neutrino

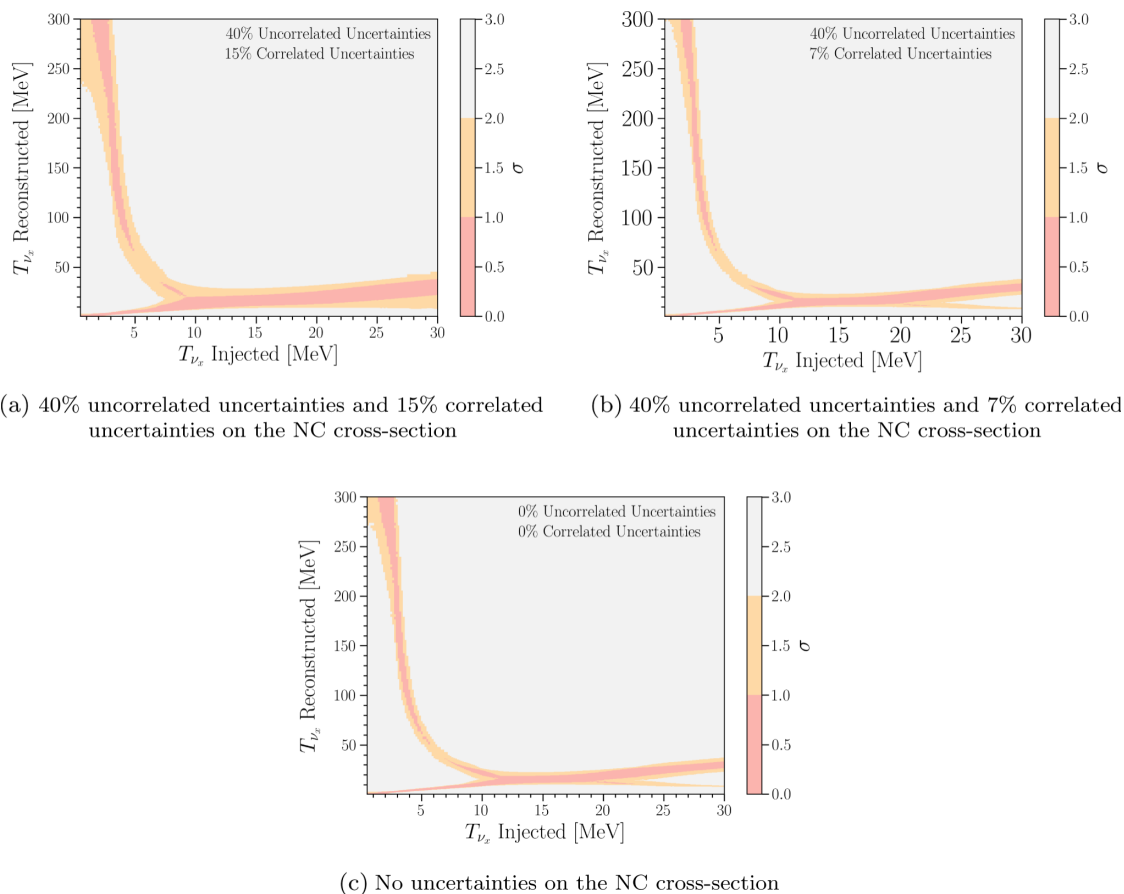


FIG. 12. Expected T_{ν_x} credible regions with a uniform prior from 0.1 to 300 MeV. The Asimov credible regions for T_{ν_x} are shown as a function of injected T_{ν_x} by the colored regions. Average neutrino temperatures of $T_{\nu_e} = 3.3$ MeV and $T_{\bar{\nu}_e} = 4.6$ MeV are assumed. The credible regions in this figure are computed with a uniform T_{ν_x} prior that extends up 300 MeV; this is in contrast to the credible regions shown in Figs. 8–10 which limited values of T_{ν_x} to be below 60 MeV.

temperatures. In the main text of this paper, we choose to apply a prior that allows only values of T_{ν_x} below 60 MeV. This is motivated by the low temperatures observed from SN1987A [23], predicted by supernova simulation studies [24], required by constraints from neutrino induced nucleosynthesis [25,26], and disfavored by diffuse supernova background searches [27]. This results in expected sensitivities that are not biased by a degeneracy that is both far outside of the range of expected supernova behavior and which would be ruled out by other measurements.

In this Appendix we show the expected sensitivities under a different prior assumption, namely a uniform prior on T_{ν_x} between 0.1 and 300 MeV. Because the degenerate region extends above 60 MeV at low ν_x temperatures and contains appreciable posterior mass, this has the effect of widening the allowed regions of T_{ν_x} that are centered on the injected T_{ν_x} . Figure 12 show the expected sensitivity to T_{ν_x} with this wider range of allowed T_{ν_x} values for the three different cross section uncertainty scenarios explored in the main text. The degenerate region below ~ 5 MeV extends up into the 100s of MeV, and below ~ 3 MeV the degenerate region begins to intersect with the prior boundary at 300 MeV.

To examine the effect of this prior we compare the width of the 1σ credible region across three scenarios: the full width derived from a uniform T_{ν_x} prior between 0.1 and 300 MeV, the width of the allowed region below 60 MeV using the same uniform T_{ν_x} prior between 0.1 and 300 MeV, and finally the width derived using the prior from the main text (a hyperbolic-tangent cutoff prior that penalizes T_{ν_x} above 60 MeV and has a 3 MeV characteristic width). Figure 13 shows the fractional width of these 1σ credible regions for the three scenarios. The solid lines

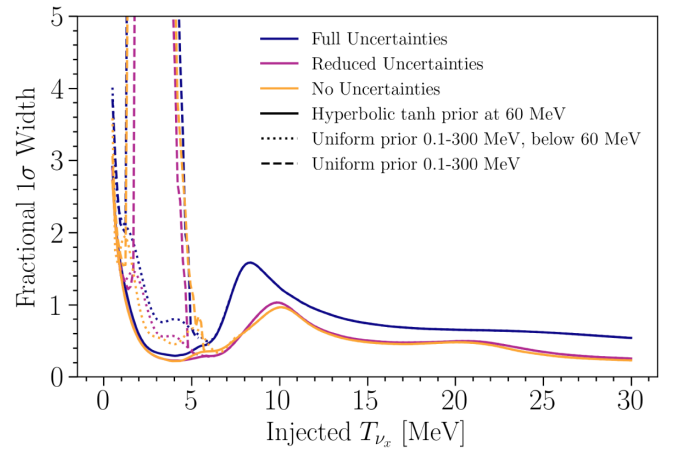


FIG. 13. Fractional width of 1σ credible regions. The solid lines correspond to the width from the hyperbolic tangent prior, the dotted lines correspond to the width below 60 MeV from the 0.1–300 MeV uniform prior, and the dashed lines correspond to the full width from the 0.1–300 MeV uniform prior (which extends up to 35). The three colors correspond to the three cases of cross section uncertainties.

denote the case where T_{ν_x} prior is in the form of a hyperbolic tangent cutoff at 60 MeV. Relaxing the prior assumptions on T_{ν_x} significantly widens the allowed regions below 60 MeV for injected T_{ν_x} between 1 and 5 MeV, but does not significantly affect the expected allowed regions outside of this region. The width of the allowed regions considering the full T_{ν_x} parameter space up to 300 remains largely unchanged outside of this 1 to 5 MeV region of injected T_{ν_x} , but between 1 and 5 MeV is dominated by the large width of the high-temperature degenerate region.

-
- [1] A. Mirizzi, I. Tamborra, H.-T. Janka, N. Saviano, K. Scholberg, R. Bollig, L. Hudepohl, and S. Chakraborty, *Riv. Nuovo Cimento* **39**, 1 (2016).
- [2] K. Hirata, T. Kajita, M. Koshiba, M. Nakahata, Y. Oyama, N. Sato, A. Suzuki, M. Takita, Y. Totsuka, T. Kifune *et al.*, *Phys. Rev. Lett.* **58**, 1490 (1987).
- [3] T. Haines, C. Bratton, D. Casper, A. Ciocio, R. Claus, M. Crouch, S. Dye, S. Errede, W. Gajewski, M. Goldhaber *et al.*, *Nucl. Instrum. Methods Phys. Res., Sect. A* **264**, 28 (1988).
- [4] E. N. Alekseev, L. N. Alekseeva, I. V. Krivosheina, and V. I. Volchenko, *Phys. Lett. B* **205**, 209 (1988).
- [5] A. A. Abud *et al.* (DUNE Collaboration), *Phys. Rev. D* **107**, 112012 (2023).
- [6] K. Abe *et al.* (Hyper-Kamiokande Collaboration), *Astrophys. J.* **916**, 15 (2021).
- [7] G. G. Raffelt, *Astrophys. J.* **561**, 890 (2001).
- [8] G. G. Raffelt, M. T. Keil, R. Buras, H.-T. Janka, and M. Rampp, in *Proceedings of the 4th Workshop on Neutrino Oscillations and their Origin (NOON2003)*, edited by Y. Suzuki, M. Nakahata, Y. Itow, M. Shiozawa, and Y. Obayashi (World Scientific, Singapore, 2003), pp. 380–387, [arXiv:astro-ph/0303226](https://arxiv.org/abs/astro-ph/0303226).
- [9] R. Buras, H.-T. Janka, M. T. Keil, G. G. Raffelt, and M. Rampp, *Astrophys. J.* **587**, 320 (2003).
- [10] W. Tornow, A. P. Tonchev, S. W. Finch, Krishichayan, X. B. Wang, A. C. Hayes, H. G. D. Yeomans, and D. A. Newmark, *Phys. Lett. B* **835**, 137576 (2022).
- [11] M. Bhattacharya, C. D. Goodman, and A. García, *Phys. Rev. C* **80**, 055501 (2009).
- [12] B. Abi *et al.* (DUNE Collaboration), [arXiv:2002.03005](https://arxiv.org/abs/2002.03005).
- [13] F. Cavanna (personal communication).
- [14] Z. Djuricic *et al.* (JUNO Collaboration), [arXiv:1508.07166](https://arxiv.org/abs/1508.07166).

- [15] T. Totani, K. Sato, H. E. Dalhed, and J. R. Wilson, *Astrophys. J.* **496**, 216 (1998).
- [16] H. Minakata, H. Nunokawa, R. Tomas, and J. W. F. Valle, *J. Cosmol. Astropart. Phys.* **12** (2008) 006.
- [17] N. F. Bell, M. J. Dolan, and S. Robles, *J. Cosmol. Astropart. Phys.* **09** (2020) 019.
- [18] K. Abe *et al.* (Hyper-Kamiokande Collaboration), [arXiv: 1805.04163](https://arxiv.org/abs/1805.04163).
- [19] K. Scholberg, *Annu. Rev. Nucl. Part. Sci.* **62**, 81 (2012).
- [20] D. Foreman-Mackey, D. W. Hogg, D. Lang, and J. Goodman, *Publ. Astron. Soc. Pac.* **125**, 306 (2013).
- [21] W. D. Voursden, W. M. Farr, and I. Mandel, *Mon. Not. R. Astron. Soc.* **455**, 1919 (2015).
- [22] J. F. Beacom, *Annu. Rev. Nucl. Part. Sci.* **60**, 439 (2010).
- [23] S. E. Woosley and W. C. Haxton, *Nature (London)* **334**, 45 (1988).
- [24] M. T. Keil, G. G. Raffelt, and H.-T. Janka, *Astrophys. J.* **590**, 971 (2003).
- [25] T. Yoshida, T. Kajino, and D. H. Hartmann, *Phys. Rev. Lett.* **94**, 231101 (2005).
- [26] A. Heger, E. Kolbe, W. C. Haxton, K. Langanke, G. Martinez-Pinedo, and S. E. Woosley, *Phys. Lett. B* **606**, 258 (2005).
- [27] H. Yuksel, S. Ando, and J. F. Beacom, *Phys. Rev. C* **74**, 015803 (2006).